Synthesis of a polyphenylacetylene/silica nanotube composite under high-temperature, high-pressure conditions

Marco Fabbiani, Jerome Rouquette, Gael Talbi, Martine Cambon, Olivier Cambon, Mario Santoro, Leszek Konczewicz, Sylvie Contreras, Julien Haines

Synthesis of a polyphenylacetylene/silica nanotube composite under high-temperature, high-pressure conditions

Marco Fabbiani, Jérôme Rouquette, Gaël Talbi, Martine Cambon, Olivier Cambon, Mario Santoro,

Leszek Konczewicz, Sylvie Contreras, Julien Haines

Marco Fabbiani, Jérôme Rouquette, Gaël Talbi, Martine Cambon, Olivier Cambon, Julien Haines.

ICGM, CNRS, Université de Montpellier, ENSCM, Montpellier, France.

Mario Santoro. Istituto Nazionale di Ottica (CNR-INO) and European Laboratory for Non Linear Spectroscopy (LENS), 50019 Sesto Fiorentino, Italy.

Leszek Konczewicz. L2C, CNRS, Université de Montpellier, Montpellier, France. Institut of High Pressure Physics, Warsaw, Poland

Sylvie Contreras. L2C, CNRS, Université de Montpellier, Montpellier, France.

Corresponding author: Julien Haines, ICGM, CNRS, Université de Montpellier, ENSCM, Montpellier, France. +33467149349 (email: Julien.Haines@umontpellier.fr).

Abstract: Phenylacetylene was inserted and polymerized in 5 nm diameter silica nanotubes under high pressure – high temperature conditions of 0.5 GPa and 437 K in an inert gas. The resulting nanocomposite was characterized by infrared and Raman spectroscopy and scanning and transmission electron microscopy. The vibrational spectroscopic data confirmed the formation of π-conjugated polyphenylacetylene and the absence of crystallization of the amorphous nanotubes. Scanning transmission electron microscopy coupled with energy dispersive x-ray spectroscopy, STEM-EDX, measurements confirmed the insertion of the polymer in the channels of the nanotubes and electron diffraction confirmed the amorphous nature of both the polymer and the host SiO_2 nanotubes. The obtained nanocomposite is a candidate material for gas sensing applications.

Keywords: silica nanotubes, polymer, high pressure, transmission electron microscopy, Raman spectroscopy

Résumé : Du phénylacétylène a été inséré puis polymérisé dans des nanotubes de silice de diamètre 5nm dans de conditions de haute pression 0,5 GPa et haute température 437K. Le nanocomposite obtenu a été caractérisé par spectroscopies infrarouge et Raman et par microscopies électronique à balayage et en transmission. Les données de spectroscopie vibrationnelle ont confirmé la formation de polyphénylacétylène π-conjugué ainsi que l'absence de cristallisation des nanotubes amorphes. La

microscopie électronique en transmission à balayage, couplée à la spectroscopie des rayons X en dispersion d'énergie a confirmé l'insertion du polymère à l'intérieur des canaux des nanotubes. La diffraction électronique a confirmé la nature amorphe du polymère et des nanotubes de SiO_2 hôte. Le nanocomposite est un candidat comme matériau pour les capteurs de gaz.

Mots-clés : nanotubes de silice, polymère, haute pression, microscopie électronique en transmission, spectroscopie Raman

Introduction

Polyphenyacetylene[1-10] has attracted particular attention over the past decades as a π-conjugated system, which can be used as a conducting polymer. Conducting polymers present a considerable interest for applications in organic electronics. These materials, including polyphenylacetylene, have been used as active layers in gas sensors[11,12]. The nanoconfinement of conducting polymers in micro- or mesoporous host materials can be used both to modify the structure and electronic properties of the polymer. The spatial constraints induced by the host material can reduce the amount of defects in the polymer, such as branched chains, and in certain cases, favor a selectivity in the polymerization reaction such that a certain isomer is obtained preferentially. In the case of the archetypical conducting polymer, polyacetylene, nanoconfinement in zeolites[13,14] can be used to selectively obtain the cis or the trans forms, which are

predicted from theory to exhibit distinct electronic properties as either a semiconductor or a metal. High-pressure is a powerful tool to ensure a high density of monomer in the pores and to favor polymerization. In a large number of unsaturated hydrocarbons, pressure can directly induce polymerization[15]. Moderate heating can also be used in conjunction with modest pressures to obtain nanoconfined polymers. In the case of the 1-D aluminophosphate $AlPO_4$-54, with 1.2 nm pores, high-pressure, high temperature conditions were used to insert phenylacetylene in the pores and induce polymerization. The resulting nanocomposite showed promising properties as a gas sensor material, in particular for water and butanol vapors[16].

On the mesoscopic scale, different types of nanotubes could be used to confine conducting polymers. In the case of carbon nanotubes, polyphenylacetylene has been used to wrap the external surface of the nanotubes[17,18]; however, carbon nanotubes are not insulators. Silica nanotubes are an interesting candidate as an insulating host material. Narrow silica nanotubes with inner diameters of between 4-6 nm can be obtained from acid treatment of chrysotile[19,20] followed by heating[21,22]. In the present study, phenylacetylene was inserted in silica nanotubes under high pressure and high-pressure, high-temperature conditions were used to form the polymer. The resulting nanocomposite was studied by scanning and transmission electron microscopy, and infrared and Raman spectroscopy.

Experimental methods

The silica nanotubes were prepared by treating pure chrysotile fibers with a nitric acid solution [21]. The resulting nanotubes were washed with distilled water and dried in air at 600 °C for 12 hours to remove water and hydroxyl groups from the internal silica walls of the nanotubes.

High-pressure experiments were performed in a high pressure bomb connected by a flexible capillary to a UNIPPRESS three-stage gas compressor using helium gas as a pressure transmitting medium . The pressure in the system was measured based on the variation of the resistance of a manganin coil placed in the main vessel of the compressor and kept at stable, room temperature independent of the temperature changes in the high pressure chamber. The 30-35 nm outer-diameter, 4-6 nm inner-diameter silica nanotubes were placed inside a 15 mm long, 3.5 mm inner diameter PTFE capsule and purified-dry phenylacetylene was added under an Ar atmosphere in the glovebox. The capsule was placed in the high pressure bomb equipped with a resistive heater, which was pressurized to 500 MPa and heated at 164°C for 90 minutes. The pressure and temperature values were based on previous work[16,23] in order that they were high enough to efficiently polymerize PhA, but low enough to avoid crystallization of the silica nanotubes. The temperature inside the heater was measured by a copper-constantan (Type T) thermocouple placed close to the capsule.

Scanning electron microscopy (SEM) was performed using a FEI Quanta 200 FEG microscope. The sample was mounted on conducting carbon adhesive tape. Transmission electron microscopy (TEM) and electron diffraction measurements were performed with FEG JEOL 2200 FS – 200 KV electron microscope equipped a CCD GATAN USC camera with 4092×4092 pixels and a 200 kV electron gun. The probe diameter in STEM mode is about 1nm with a resolution, which can reach 1Å. The sample was incorporated in IR-white Resin (Sigma Aldrich) and cut into 70 nm slices using ultramicrotomy.

IR measurements on the recovered PPhA/SiO_2 nanocomposite sample, SiO_2 nanotubes and PhA (in CCl_4 solvent) were performed on a Bruker Tensor 27 FT-IR spectrometer using an attenuated total reflectance (ATR) accessory. Raman spectra were obtained using a Horiba Jobin-Yvon LabRam Aramis Raman spectrometer equipped with a near infrared diode laser (λ = 785 nm), a BX41 confocal Olympus microscope (50x / N.A. 0.50 objective), and a Peltier-cooled charge coupled device camera and a Renishaw inVia confocal raman microscope equipped with a near infrared diode laser (λ = 785 nm) and a Leica microscope with a 50x objective. The laser power was about 1-20 mW on the sample. The position of the focal point of the laser beam inside the sample was about 10 μm from the surface. The diameter of the laser beam was about 10 μm.

Results and discussion

After the pressure-temperature treatment at 500 MPa and 164°C, the product obtained was recovered as an orange powder. The resulting sample was investigated by SEM, Fig. 1. It consisted of small and large bundles of nanotubes, of up to 25 μm long and a few microns in diameter, embedded in bulk polyphenylacetylene (PPhA), see IR and Raman results in the following section. Energy dispersive x-ray analysis, Fig. 2, indicated that carbon was present throughout the sample, whereas the silicon-containing regions corresponded to the nanotubes in the SEM image. The carbon corresponds to bulk PPhA and the regions containing carbon and silicon potentially correspond to PPhA-filled silica nanotubes. Confirmation of this hypothesis required the higher spatial resolution of transmission electron microscopy.

Regions were identified in the TEM images, Fig. 3, corresponding to the cross-section of the nanotubes with lighter circular regions that are compatible with a central pore of 4-6 Å. The typical EDX spectrum, Fig. 4, obtained from this type of region confirms the presence of C, Si and O, which is consistent with a PPhA filled silica nanotube. The lighter and darker regions were also investigated by electron diffraction,

Fig. 5. In both cases amorphous-type diffraction patterns were observed. This indicates that the high-pressure, high temperature conditions applied were not sufficient to induce crystallization of the silica nanotubes. It can also be concluded that the inserted PPhA is amorphous.

The infrared spectrum of the nanocomposite, Fig. 6, contains a series of modes in the C-H stretching region, the C=C stretching region and at lower wavenumbers bending vibrations of the hydrocarbon, Table 1. The observed modes are in good agreement with previous work on PPhA[1,2,4-6,9,10]. The C(sp)-H stretching modes near 3300 cm^{-1}, which are very strong in the PhA monomer, are very weak in the nanocomposite. This indicates that only a very small amount of monomer remains. The C(sp^2)-H stretching modes between 3021 and 3078 cm^{-1} correspond to the vinyl and phenyl groups of PPhA. The weak C(sp^3)-H stretching modes just below 3000 cm^{-1} indicates the presence of defects due to, for example, branched chains or terminal groups. In addition to the contributions of PPhA, a broad shoulder and two strong broad bands due to the silica nanotubes are observed at 1188, 1063 and 445 cm^{-1}. These modes correspond to νSi-O and δSi-O-Si vibrations of the amorphous SiO_2 nanotubes, respectively[20]. An additional Si-O band at 802 cm^{-1} has been related to distortion of the SiO_4 tetrahedra. It can be noted that no signals from hydroxyl groups or water are present, indicating that the nanotubes correspond to anhydrous silica. The Raman spectrum, Fig.7, is consistent with previous results on PPhA[3]. The strongly colored PPhA/silica nanotube composite exhibited strong fluorescence in the visible region of the spectrum. This required the use of the near infrared diode laser (λ = 785 nm) for the Raman spectroscopic measurements. In the Raman spectrum from the literature of the monomer, the C≡C stretching vibration near 2100 cm^{-1} is particularly intense[24]. In contrast, this mode is particularly weak in the spectrum of the nanocomposite thereby confirming that very little monomer remains. The lower frequency modes of the C=C stretching vibrations and those of the phenyl groups are particularly prominent, Table 1. The spectroscopic results are consistent with previous data for polyphenylacetylene[1,2,4-6,9,10], indicating that the interaction between the PPhA and the walls of the silica nanotubes is of the weak van der Waal's type.

In comparison with monomeric PhA, the relative intensities of the characteristic C^{sp}-H (Fig. 6) and C≡C (Fig. 7) stretching modes of the monomer with respect to modes arising from the phenyl groups, which are retained on polymerization, decrease by more than an order of magnitude in the spectra of the PPhA/silica nanotube composite indicating only trace amounts of monomer remain after HP-HT treatment.

The combination of the electron microscopy and vibrational spectroscopy results indicate that the nanocomposite consists of anhydrous amorphous silica nanotubes filled with amorphous polyphenylacetylene in a bulk PPhA matrix. Such a material is a potential candidate for gas sensor applications as was found in the case of PPhA/$AlPO_4$-54 with smaller 1.2 nm pores. The different pore size and the chemical and hydrophilic/hydrophobic nature of the porous material, silica versus $AlPO_4$, will certainly modify the interactions with various gaseous species providing complementary gas sensing properties with different sensitivities to each chemical species, when placed on quartz crystal microbalances. Complementary nanocomposite materials can be of interest in the fabrication of electronic noses.

Conclusions

Phenylacetylene was inserted and polymerized in silica nanotubes under high-pressure, high temperature conditions. The resulting nanocomposite was investigated by scanning and transmission electron microscopy and infrared and Raman spectroscopy. The results of these combined techniques

indicated that the phenylacetylene monomer was essentially fully consumed during the HP-HT treatment, producing a polymer that both filled the 4-6 nm diameter silica nanotubes and was present as a bulk phase surrounding the nanotubes. Both the silica nanotubes and the polyphenylacetylene are amorphous and the nanocomposite is anhydrous. This material may be of considerable interest for gas sensor applications.

Table 1: IR and Raman modes for the PPhA/SiO_2 nanocomposite. Detailed assignements for PPhA and PhA can be found elsewhere[1-6,9,10,24].

IR Wavenumber (cm^{-1})	Raman Shift (cm^{-1})	Assignment
3303		C-H sp
3280		C-H sp
3078		C-H sp^2
3052		C-H sp^2
3021		C-H sp^2
2924		C-H sp^3
2854		C-H sp^3
	2109	C≡C
	1626	C=C
1596	1600	C=C, C-ϕ
1575	1580	C=C
	1500	C=C phenyl
1490	1494	C=C phenyl
	1460	C=C phenyl
1442	1446	C=C phenyl
1412		PPhA
1390		
	1362	C-C
	1348	C-C
	1314	phenyl
	1291	C-H shear
	1276	C-H shear
	1249	
	1235	PPhA overtone
	1194	C-ϕ
1188 (shoulder)		νSi-O
1178	1178	C-H bend
1152	1158	C-H bend
1091		
1070		phenyl
1063		νSi-O
1029	1032	phenyl
1001	1001	phenyl
983	981	PPhA
965	967	PPhA
910	917	PPhA
	896	
879	874	PPhA
837	843	PPhA
802		Si-O
751	763	PPhA
	717	
692	697	PPhA
629	619	PPhA
610	610	PPhA
568		PPhA
560		
545		
529	529	
	520	
465	466	PPhA

445		δSi-O-Si
	405	PPhA
	236	

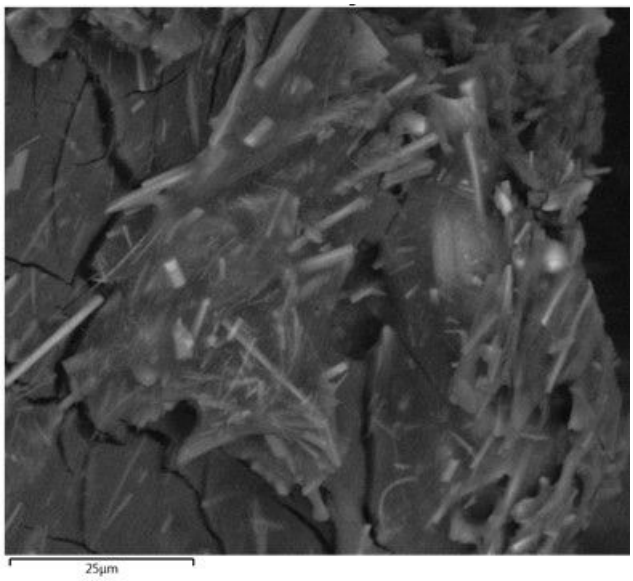

Fig. 1. Scanning electron micrograph of the PPhA/SiO_2 nanocomposite.

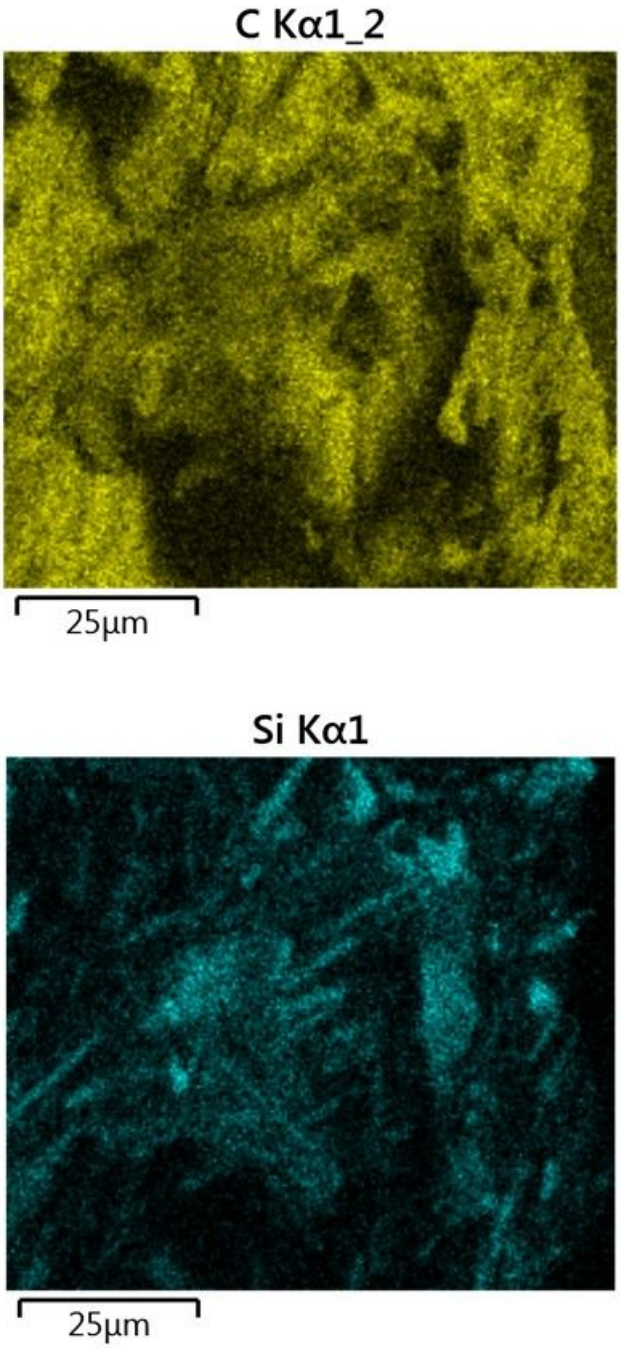

Fig. 2. SEM-EDX images of the PPhA/SiO_2 nanocomposite.

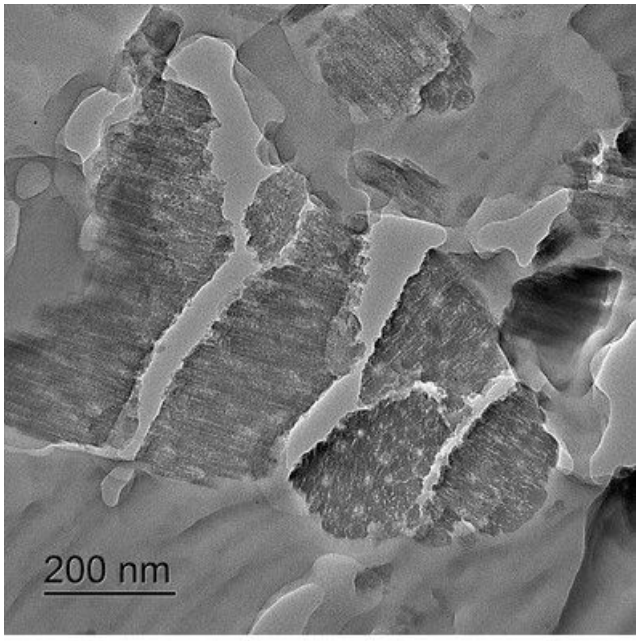
200 nm

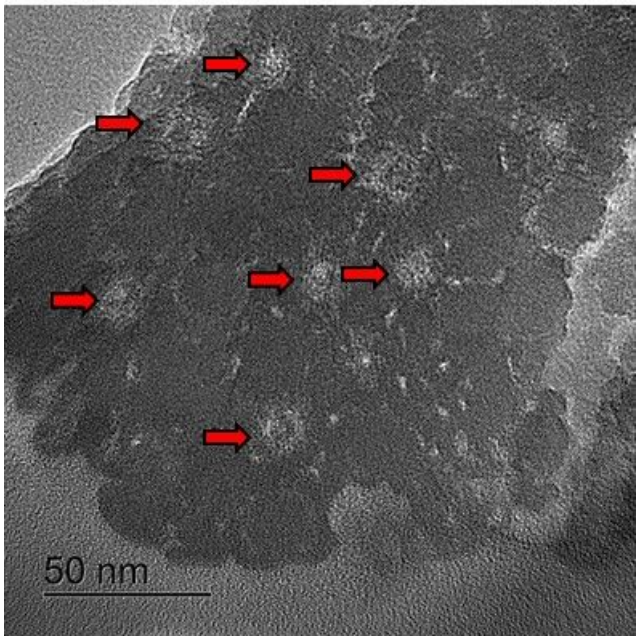
50 nm

Fig. 3. Transmission electron micrographs of the PPhA/SiO_2 nanocomposite. The circular channels at the centers of the nanotubes are indicated by arrows.

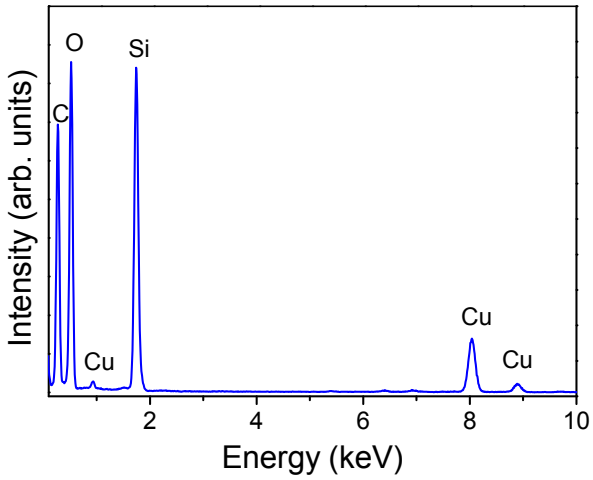

Fig. 4. STEM-EDX spectrum in the circular light-colored zone of the PPhA/SiO_2 nanocomposite. The copper peaks are due to the TEM sample grid.

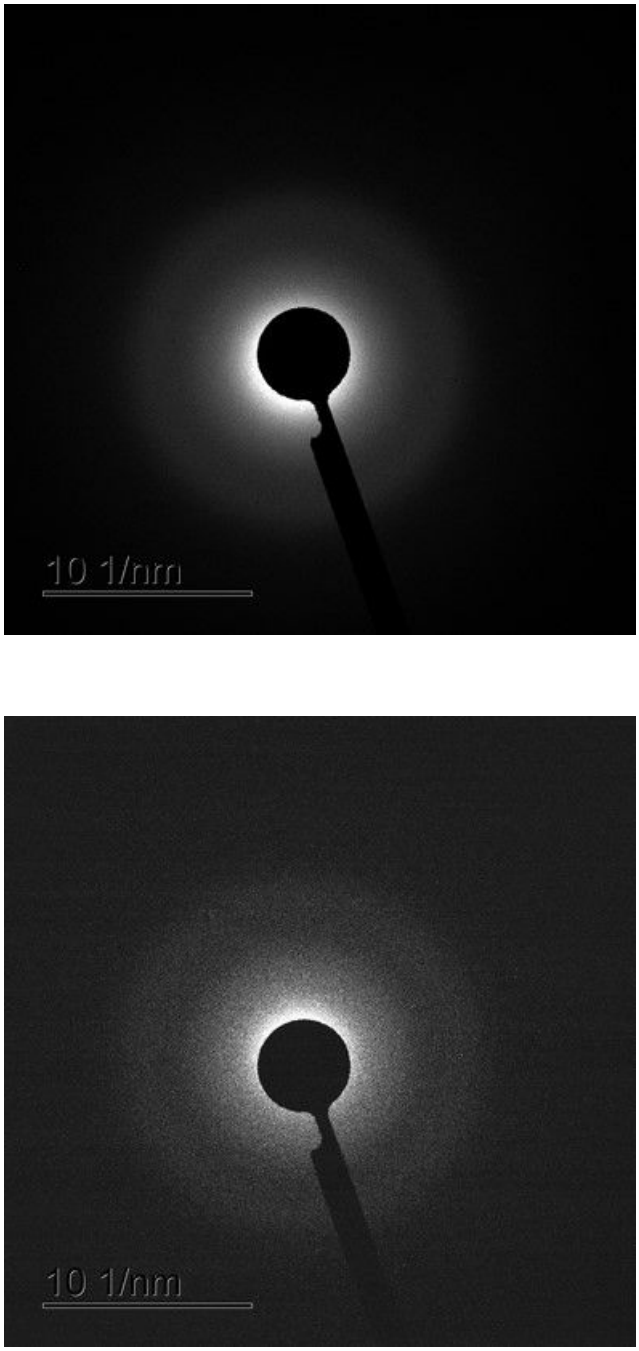

Fig. 5. Electron diffraction of the dark (above) and lighter circular (below) zones of the PPhA/SiO_2 nanocomposite.

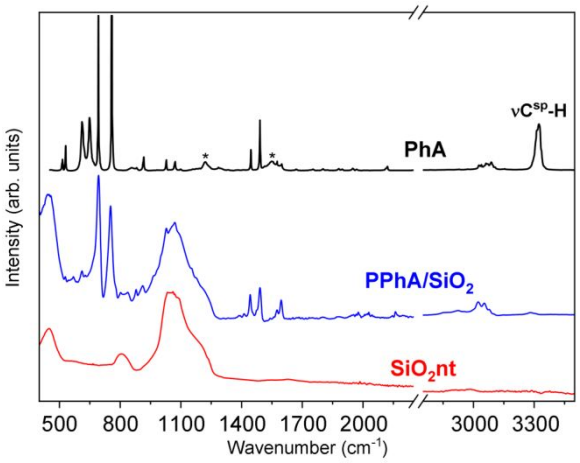

Fig. 6. Attenuated total reflectance infrared spectrum of PhA, silica nanotubes (SiO_2nt) and the PPhA/SiO_2 nanocomposite. (*) Solvent signals from CCl_4.

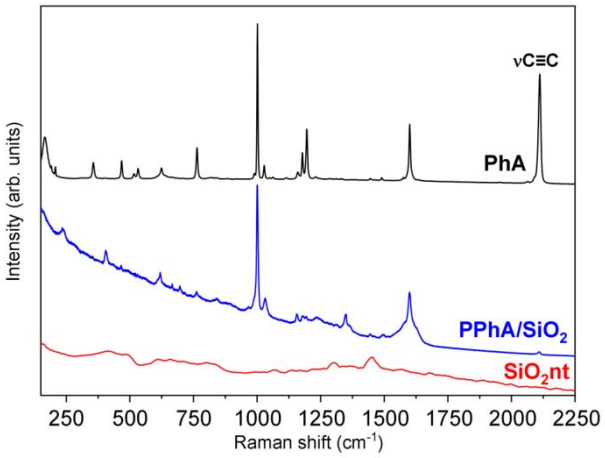

Fig. 7. Raman spectrum of PhA, silica nanotubes (SiO_2nt) and the PPhA/SiO_2 nanocomposite. The grating used limited acquisition to below 2300 cm^{-1}.

Acknowledgments

We would like to thank Véronique Viguier, Frédéric Fernandez and Erwan Oliviero from the "Plateforme de Microsocpie Electronique et Analytique" and David Maurin from the "Plateforme Technologique de Spectroscopie Vibrationnelle IR-Raman" of the Université de Montpellier and Léa Daenens from the "Plateforme d'Analyse et de Caractérisation" of the ICGM.

REFERENCES

(1) Kern, R. J. *Journal of Polymer Science Part a-1-Polymer Chemistry* **1969**, *7*, 621.

(2) Masuda, T.; Sasaki, N.; Higashimura, T. *Macromolecules* **1975**, *8*, 717.

(3) Bloor, D. *Chem Phys Lett* **1976**, *43*, 270.

(4) Simionescu, C.; Dumitrescu, S.; Percec, V. *J Polym Sci Pol Sym* **1978**, 209.

(5) Chauser, M. G.; Koltsova, L. S.; Vladimirov, L. V.; Urman, Y. G.; Alekseeva, S. G.; Zaichenko, N. L.; Oleinik, E. F.; Cherkashin, M. I. *Vysokomolekulyarnye Soedineniya Seriya A* **1988**, *30*, 1464.

(6) Gruzdeva, V. F.; Bondarenko, G. N.; Prokofeva, N. I.; Gribov, L. A. *Vysokomolekulyarnye Soedineniya Seriya A* **1989**, *31*, 748.

(7) Hirao, K.; Ishii, Y.; Terao, T.; Kishimoto, Y.; Miyatake, T.; Ikariya, T.; Noyori, R. *Macromolecules* **1998**, *31*, 3405.

(8) Ishii, F.; Matsunami, S.; Shibata, M.; Kakuchi, T. *Journal of Polymer Science Part B-Polymer Physics* **1999**, *37*, 1657.

(9) Vosloo, H. C. M.; Duplessis, J. A. K. *Polym. Bull.* **1993**, *30*, 273.

(10) Vosloo, H. C. M.; Luyt, A. S. *J. Therm. Anal. Calorim.* **1995**, *44*, 1261.

(11) Bearzotti, A.; Foglietti, V.; Polzonetti, G.; Iucci, G.; Furlani, A.; Russo, M. V. *Mat Sci Eng B-Solid* **1996**, *40*, 1.

(12) Bearzotti, A.; Macagnano, A.; Pantalei, S.; Zampetti, E.; Venditti, I.; Fratoddi, I.; Russo, M. V. *J Phys-Condens Mat* **2008**, *20*.

(13) Scelta, D.; Ceppatelli, M.; Santoro, M.; Bini, R.; Gorelli, F. A.; Perucchi, A.; Mezouar, M.; van der Lee, A.; Haines, J. *Chem Mater* **2014**, *26*, 2249.

(14) Santoro, M.; Scelta, D.; Dziubek, K.; Ceppatelli, M.; Gorelli, F. A.; Bini, R.; Garbarino, G.; Thibaud, J.-M.; Di Renzo, F.; Cambon, O.; Hermet, P.; Rouquette, J.; van der Lee, A.; Haines, J. *Chem Mater* **2016**, *28*, 4065.

(15) Santoro, M.; Ciabini, L.; Bini, R.; Schettino, V. *J. Raman Spectrosc.* **2003**, *34*, 557.

(16) Frederico G. Alabarse, M. P., Marco Fabbiani, Simona Quartieri, Rossella Arletti,; Boby Joseph, F. C., Sylvie Contreras, Leszek Konczewicz, Jerome Rouquette,; Bruno Alonso, F. D. R., Giulia Zambotti, Marco Baù, Marco Ferrari, Vittorio Ferrari,; Andrea Ponzoni, M. S., Julien Haines *ACS Appl. Mater. Interfaces* **2021**, *13*, 27237−27244.

(17) Tang, B. Z.; Xu, H. Y. *Macromolecules* **1999**, *32*, 2569.

(18) Liu, X. Q.; Li, Y. L.; Lin, Y. W.; Yang, S.; Guo, X. F.; Li, Y.; Yang, J.; Chent, E. Q. *Macromolecules* **2013**, *46*, 8479.

(19) Wang, L. J.; Lu, A. H.; Wang, C. Q.; Zheng, X. S.; Zhao, D. J.; Liu, R. *J. Colloid Interface Sci.* **2006**, *295*, 436.

(20) Liu, K.; Feng, Q. M.; Yang, Y. X.; Zhang, G. F.; Ou, L. M.; Lu, Y. P. *J. Non-Cryst. Solids* **2007**, *353*, 1534.

(21) TALBI, G.; CAMBON, O.; CAMBON, M.; B09B 3/00 (2006.01) ,A62D 101/41 (2007.01) ed. 2019; Vol. WO/2019/038502.

(22) Talbi, G.; Cambon, M.; Cambon, O. *J. Mater. Cycles Waste Manag.* **2019**, *21*, 1167.

(23) Zhao, Y. X.; Talbi, G.; Clement, S.; Toulemonde, P.; Hansen, T.; Cambon, M.; Cambon, O.; Beaudhuin, M.; Viennois, R.; Haines, J. *Solid State Sci* **2020**, *101*.

(24) Chernia, Z.; Livneh, T.; Pri-Bar, I.; Koresh, J. E. *Vib Spectrosc* **2001**, *25*, 119.